



Cite this: *RSC Adv.*, 2015, 5, 102904

# Proton-assisted low-temperature sintering of Cu fine particles stabilized by a proton-initiating degradable polymer†

Masaki Matsubara,<sup>‡a</sup> Tetsu Yonezawa,<sup>\*a</sup> Takato Minoshima,<sup>a</sup> Hiroki Tsukamoto,<sup>a</sup> Yingqiong Yong,<sup>a</sup> Yohei Ishida,<sup>a</sup> Mai Thanh Nguyen,<sup>a</sup> Hiroki Tanaka,<sup>b</sup> Kazuki Okamoto<sup>b</sup> and Takuya Osaka<sup>b</sup>

Metallic copper fine particles were prepared by chemical reduction of CuO in the presence of thermally degradable poly-1,4-butanediol-divinylether (BDVE). Because a BDVE thin layer formed on the particle surfaces, the obtained copper particles were stable and did not undergo obvious oxidation under ambient conditions. The ether groups of BDVE were hydrolyzed with protons, and this generated small fragment molecules. The BDVE-stabilized copper fine particles and their pastes can be therefore sintered at 150 °C in the presence of protons. Electro-conductive films with a relatively low resistivity of  $8.5 \times 10^{-5} \Omega \text{ cm}$  were obtained on a alumina substrate in the presence of formic acid, and hot pressed conductive pellets with a resistivity of  $2.9 \times 10^{-5} \Omega \text{ cm}$  were also obtained without any pre-oxidative annealing in the presence of proton generator molecules at very low temperatures. The hot pressed pellets show a high anti-oxidative ability and their corrosion tests revealed their good anti-corrosion property.

Received 15th October 2015  
 Accepted 23rd November 2015

DOI: 10.1039/c5ra21402e

[www.rsc.org/advances](http://www.rsc.org/advances)

## Introduction

Metal nanoparticles and fine particles have attracted extensive attention in nanotechnology<sup>1–5</sup> as well as in electronics.<sup>6–8</sup> In particular, conductive inks and pastes containing a high concentration of metal nanoparticles and fine particles are important candidates for production of printed electronics<sup>9–12</sup> that are currently in demand. This is because of their potential applications in low cost wet processes, especially for producing flexible devices, including organic devices. So far, gold<sup>13–15</sup> and silver<sup>16–19</sup> pastes and inks have been frequently applied for producing electro-conductive films and patterns owing to their high stability and low resistivity. However, the cost of precious metals inhibits their economical use and electromigration of silver has been a major issue impeding their application. Copper is a preferable alternative to gold and silver from the viewpoint of cost and electromigration issues. Copper is

a common element, and it has a high electroconductivity. Moreover, it is not magnetic. Many efforts on the use of inks and pastes of copper particles<sup>20–34</sup> and copper organo-complexes<sup>35–39</sup> have been made to develop low-temperature sintering processes including photo and laser irradiation sintering.<sup>40–42</sup> However, copper fine particles get oxidized easily even under ambient conditions and this problem limits their application.

In order to overcome this oxidation issue, protection of copper particle surfaces against oxidation is of immediate importance.<sup>20–34</sup> Polymers,<sup>20–27</sup> surfactants,<sup>28–31</sup> including alkylamines,<sup>31</sup> and metal,<sup>32</sup> and metal oxide<sup>33</sup> shells have been used as an anti-oxidation layer on the particle surfaces. In most cases, however, the introduction of an anti-oxidation layer on copper particles means the formation of a non-conductive layer, such as an organic layer and a metal oxide layer, on the surface of particles. The only exception is the formation of a metallic layer composed of noble metal elements on copper particle surfaces. However, such noble-metal layers are costly. Further, metal oxides cannot be eliminated from the obtained layers by thermal sintering. In contrast, polymers are good candidates for protecting the surface of copper particles against oxidation,<sup>20–27</sup> and may be decomposed during sintering. For use in electro-circuits, direct metal–metal contacts in the particle layers must be obtained during sintering processes to realize better electro-conductivity. However, organic polymers usually do not evaporate even at high temperatures but directly begin to decompose at  $\sim 400 \text{ }^\circ\text{C}$ , and polymer-stabilized metal particles need to be subjected to high-temperature sintering<sup>8</sup> or laser

<sup>a</sup>Division of Materials Science and Engineering, Faculty of Engineering, Hokkaido University, Kita 13 Nishi 8, Kita-ku, Sapporo, Hokkaido 060-8628, Japan. E-mail: [tetsu@eng.hokudai.ac.jp](mailto:tetsu@eng.hokudai.ac.jp)

<sup>b</sup>Corporate Research Center, Daicel Corporation, 1239, Shinzaike, Aboshi-ku, Himeji, Hyogo 671-1283, Japan

† Electronic Supplementary Information (ESI) available: Schematic illustration of the electro-conductivity measurement. TGA cart of Cu fine particles. SEM image of the Cu pellets obtained by hot-pressing. See DOI: 10.1039/c5ra21402e

‡ Present address: Department of Materials and Environmental Engineering, National Institute of Technology, Sendai College, 48 Nodayama, Medeshima-Shiote, Natori 981-1239, Japan.



irradiation<sup>42</sup> to remove polymers. We have demonstrated that oxidative sintering can form copper oxide dots on the particle surface and these dots change to metallic necking under reductive sintering.<sup>26,27,31</sup> However, this two-step sintering process involves quite a long sintering time of 8 hours. From this point of view, decomposition of the stabilizing polymer molecules at a moderate temperature into small fragments that can be evaporated or eliminated is favourable for low-temperature sintering with a shorter time. Some polymers used in biomedical applications can be decomposed into monomer species or small fragments in the presence of protons at biocompatible temperature.<sup>43–45</sup> These polymers can be used to stabilize copper fine particles in electro-conductive pastes and joining materials for low-temperature sintering. As joining materials, these degradable polymer-stabilized Cu particles also have a good potential because lead-free solder alloy<sup>46</sup> has a higher melting point, limiting its use in manufacturing of electro-circuits.

In this paper, for the first time, we present a novel strategy of low-temperature sintering of novel proton-assisted degradable polymer-stabilized copper fine particles in which the polymer can undergo proton-assisted degradation. Protons facilitated the hydrolysis of ether bonds in the main chain of polymers, resulting in small fragments. Cu conductive pellets were obtained by hot-pressing in the presence of a thermal proton generator, and the Cu conductive films were obtained by annealing in a reductive atmosphere with formic acid as a proton donor. The polymer decomposition by protons is the key factor to achieve good electro-conductivity. The difference between favourable proton generators of pellets and films will also be discussed.

## Experimental

### Materials

CuO microparticles ( $\sim 0.9 \mu\text{m}$ ) used as the metal source were supplied by Nisshin Chemco (Japan). Hydrazine monohydrate as a reducing reagent, tetrahydrofuran (THF), and ethanol were purchased from Junsei (Japan). Formic acid was obtained from Kanto (Japan). Poly-1,4-butanediol divinyl ether (BDVE, MW = ca. 9000) was synthesized by Daicel. Benzyl 4-hydroxyphenyl methyl sulfonium hexafluoroantimonate (BPMS) was used as the thermal proton generator (Scheme 1).

### Preparation of polymer-stabilized Cu fine particles

The synthetic procedure of BDVE-stabilized Cu fine particles is similar to the previously reported<sup>24,26</sup> and as follows: 0.33 g of BDVE was dissolved in 20 cm<sup>3</sup> of THF in a round-bottom flask, and then 4.0 g of CuO microparticles were dispersed into this

solution. 1.25 cm<sup>3</sup> of hydrazine monohydrate (N<sub>2</sub>H<sub>4</sub>·H<sub>2</sub>O) was added into the mixture at 50 °C, and the mixed dispersion was stirred for 2 h. After reduction, the brown precipitates were collected by decantation, and then washed 4 times with ethanol by centrifugation, and then drying at room temperature under N<sub>2</sub>. Finally, 3.1 g of Cu fine particle powder was obtained.

Larger-scale production of BDVE-stabilized Cu fine particles was also performed. For the purpose of scale up, we chose ethanol as the solvent instead of THF due to its low cost, and set the reaction temperature to 78 °C. 1.32 g of BDVE was dissolved into 200 cm<sup>3</sup> of ethanol in a round bottom flask with a reflux condenser. 16 g of CuO microparticles was dispersed into this solution. Then, this solution was refluxed at 78 °C with stirring at 800 rpm. For the complete reduction of the large amount of CuO, an excess amount of hydrazine monohydrate (50 cm<sup>3</sup>) was introduced into this mixture. An explosive boiling of the reaction mixture occurred once soon after addition of hydrazine. After stirring for 2 h, Cu fine particles were collected by decantation, and then washed 4 times with ethanol by centrifugation. 13.0 g of BDVE-stabilized Cu fine particle powder was obtained in the large-scale synthesis.

### Preparation of conductive Cu pellets at high pressure

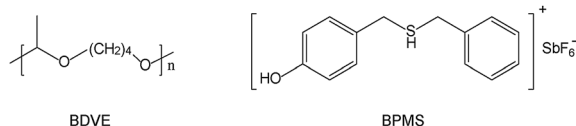
Preparation of Cu conductive pellets at high pressure is as follows: well-mixed 1.0 g of Cu particle powder prepared as described above and 10 mg of BPMS as the proton generator were introduced into a stainless vessel with diameter of 13 mm and then compacted for 30 min by a hot press machine (AH-2003, AS ONE Corp.) at 100 MPa at various temperatures (25, 80, and 100 °C) under air.

### Preparation of Cu ink and conductive Cu film

In order to prepare the ink with dispersing Cu fine particles, the obtained Cu-particle powder was first ground by using an automatic mortar for 30 min and then pulverized by using a blender. Then, the mixture was dispersed in ethanol and  $\alpha$ -terpineol using a mixer and an emulsifier. Ethanol was removed from the mixture by evaporation under vacuum and the copper content of the obtained ink was controlled as 50 wt%. Into this ink, 10 wt% of formic acid as the proton generator was added. The obtained Cu ink was then immediately deposited on a glass and an aluminum oxide (Al<sub>2</sub>O<sub>3</sub>) substrate by the doctor blade method to obtain a film with a thickness of 40  $\mu\text{m}$  and a width of 20 mm. After drying under N<sub>2</sub> for 1 h at 40 °C, the substrates were cut into 20 mm  $\times$  20 mm pieces and annealed at 150 °C in 3% H<sub>2</sub> in N<sub>2</sub> gas flow (2 dm<sup>3</sup> min<sup>-1</sup>) for 2 h. The Cu ink including 1 wt% of BPMS was also prepared and sintered in the same way.

### Characterization

Scanning electron microscope (SEM) observations of the particles were performed by using a JEOL JSM-6701F field emission SEM with an acceleration voltage of 15 kV. X-ray diffraction (XRD) patterns were obtained with a Rigaku Mini Flex II (Cu K $\alpha$ ). The thermal properties of BDVE and Cu fine particles were measured by thermogravimetric analysis (TGA) and differential



Scheme 1



thermal analysis (DTA) with a Shimadzu DTG-60H. TGA-DTA curves were obtained under air with a heating rate of 1 or 5 °C min<sup>-1</sup>. The pellet sample was pulverized into powder before TGA-DTA measurement. The sheet resistance of the copper films and pellets were obtained using a four-point probe method. In order to obtain reproducible data, six points for films and four points for pellets were measured with a four point probe, as shown in Fig. S1,† and the average values are displayed. Corrosion tests of the conductive Cu pellets were carried out in the condition of 85 °C and 85% relative humidity for 8 days using an ESPEC (Japan) SH-240 temperature and humidity testing chamber.

## Results and discussion

### Preparation and characterization of the BDVE-stabilized Cu fine particles

BDVE-stabilized Cu fine particles with a nearly spherical shape were prepared by chemical reduction of CuO micro-particles in the presence of BDVE. The average particle size was 110 ± 45 nm, as shown in Fig. 1a. We could also obtain the Cu particles of the same quality even if they were produced on a large scale with different solvents and reaction temperature. In the case of the large-scale production, the average particle size and distribution was 110 ± 38 nm, as shown in Fig. 1b. The XRD measurement results shown in Fig. 1c indicate that our Cu fine particles were not oxidized under ambient conditions for at

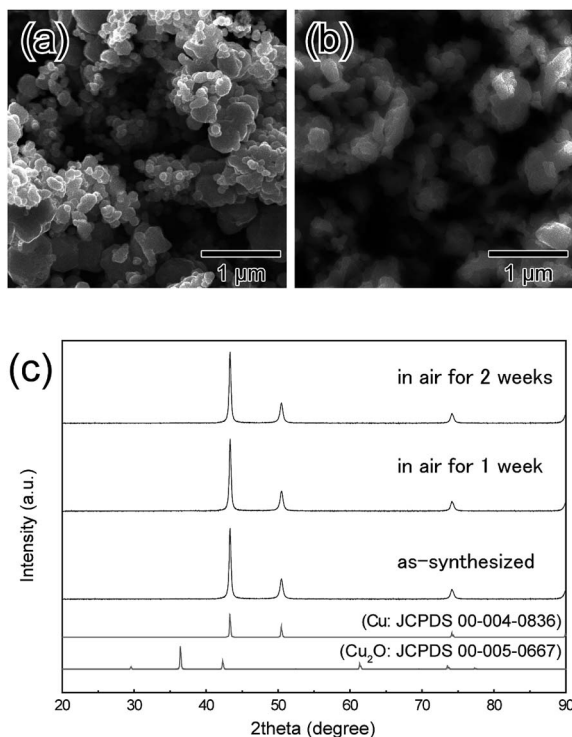


Fig. 1 (a) SEM image of as-synthesized BDVE (poly-1,4-butane-dioldivinylether)-stabilized Cu fine particles. (b) SEM image of the particles produced on the large scale. (c) XRD patterns of BDVE-stabilized Cu fine particles. Measurements were performed with the particles as prepared and stored in air for 1 and 2 weeks.

least 2 weeks and that our Cu fine particles produced on a large scale also were not oxidized under the same ambient condition at least 3 weeks. Thus, BDVE layers on the surface of Cu fine particles can prevent particle surface oxidation. As observed in the SEM image, the particle size is not quite uniform, unfortunately. In our previous study, when gelatin was used as the stabilizing polymer for Cu fine particles for similar-size, which were also prepared by hydrazine reduction of CuO micro-particles, the particles were almost spherical and the size distribution was more uniform.<sup>24,26</sup> This can be probably attributed to amino, carboxylic acid and thiol groups that can coordinate to copper atoms on the particle surface. Such strong coordination between polymer molecules and particle surface enable good control of the particle sizes and structure. In contrast, BDVE has no such coordinative groups in the polymer chain.

In order to estimate the amount of BDVE attached on the surface of Cu fine particles, TGA-DTA measurement was carried out in air (Fig. 2). The mass in the thermogram began to slightly increase at *ca.* 87 °C (see Fig. S2†), indicating that Cu began to be gradually oxidized to change into Cu<sub>2</sub>O. The DTA curve indicates that above *ca.* 177 °C, Cu<sub>2</sub>O began to be oxidized to CuO. At the end of the measurement, Cu was completely oxidized to CuO. The value of 124.3 wt% also includes the weight loss of decomposed BDVE. The initial Cu ratio of as-synthesized Cu particles can be calculated as 1.243/1.252 = 0.993 with use of the ratio of MW(CuO)/MW(Cu) = 79.545/63.546 = 1.252. From this calculation, we can estimate that the actual amount of BDVE on the surface of Cu particles is 0.7 wt%.

### Pyrolysis behaviors of BDVE with and without acids

Fig. 3 shows the pyrolysis behaviors of BDVE with and without acids. TGA measurements were carried out under air flow (200 cm<sup>3</sup> min<sup>-1</sup>) at the heating rate of 1 °C min<sup>-1</sup>. Thermal decomposition of BDVE began at *ca.* 180 °C in the absence of acids. In the presence of acids, it is expected that BDVE may decompose to lighter fragments that will be vaporized easily

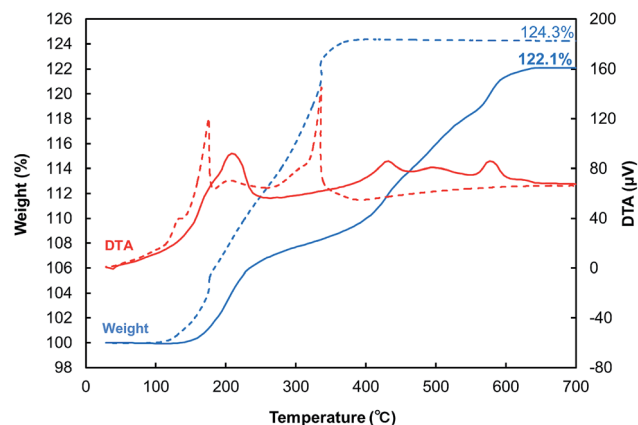


Fig. 2 TGA (blue)-DTA (red) curves of BDVE-stabilized Cu fine particles (dashed line) and Cu pellet pressed at 100 °C (solid line). The pellet was pulverized into powder before the measurement.



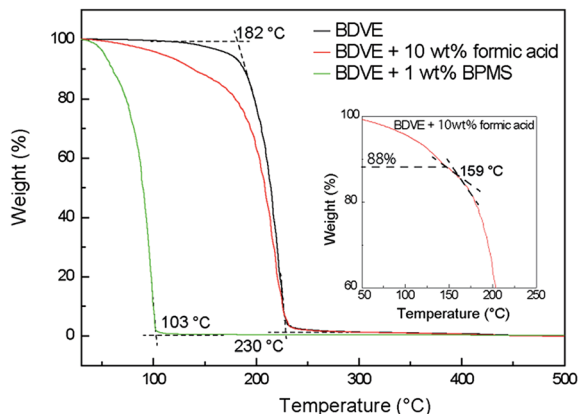


Fig. 3 TGA charts of BDVE with and without acids. TG measurements were carried out under air flow ( $200 \text{ cm}^3 \text{ min}^{-1}$ ) at the heating rate of  $1 \text{ }^\circ\text{C min}^{-1}$ . (black line) BDVE without acids. (red line) BDVE with 10 wt% of formic acid. (green line) BDVE with 1 wt% of BPMS. (Inset) Magnified curve of BDVE with 10 wt% of formic acid.

because acids promote the hydrolysis of ether bonds in the structure of BDVE. The decomposition when 10 wt% of formic acids was added can be divided into two stages. Firstly, 12 wt% of decrease in mass between 30 to  $140 \text{ }^\circ\text{C}$  could be attributed to a large amount of evaporated formic acid (b.p. =  $100.8 \text{ }^\circ\text{C}$ ), which was supposed to be 10 wt%, as well as a small amount of decomposed BDVE fragments. Next, weight decrease, indicating degradation of BDVE, started at  $159 \text{ }^\circ\text{C}$  (shown in inset of Fig. 3). BDVE underwent partial hydrolysis and changed into the evaporable pieces by formic acids during gradual evaporation of formic acid.

In the field of controlled polymerization, heat-sensitive and photosensitive proton generators are often used for initiating polymerization. BPMS is one of such heat-sensitive proton generators. BPMS can be degraded at  $100 \text{ }^\circ\text{C}$  to release protons. In this study, BPMS was used not as the polymerization initiator but as the BDVE degradation initiator. As can be observed in Fig. 3, evaporation of fragment products began at around  $100 \text{ }^\circ\text{C}$ .

### Preparation of Cu conductive pellets *via* hot-pressing

BDVE-stabilized Cu particles were pressed in air at 100 MPa for 30 min at various temperatures ( $25$ ,  $80$ , and  $100 \text{ }^\circ\text{C}$ ). The Cu pellets were 13 mm in diameter and 1 mm in thickness irrespective of the hot-pressing temperature. The obtained resistivities of the hot-pressed Cu pellets are summarized in Fig. 4a. The Cu pellet pressed at  $25 \text{ }^\circ\text{C}$  showed the resistivity of  $4.1 \times 10^{-4} \text{ } \Omega \text{ cm}$ . This indicates that some inter-particle contacts were generated by high-pressure pressing. Polymer molecules may be sufficiently flexible to move on the particle surface. The resistivity of the pellet compacted at  $80 \text{ }^\circ\text{C}$  decreased to  $1.4 \times 10^{-4} \text{ } \Omega \text{ cm}$ , suggesting that heating promotes more rapid movement of BDVE molecules. Resistivity of the pellet prepared at  $100 \text{ }^\circ\text{C}$  remained  $1.4 \times 10^{-4} \text{ } \Omega \text{ cm}$ , unfortunately, since the decomposition of BDVE does not proceed under the current temperature.

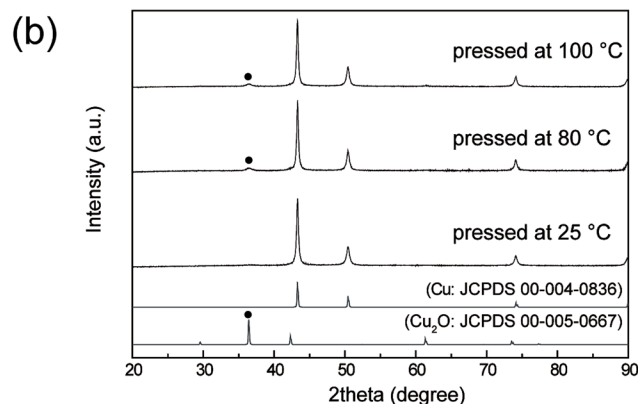
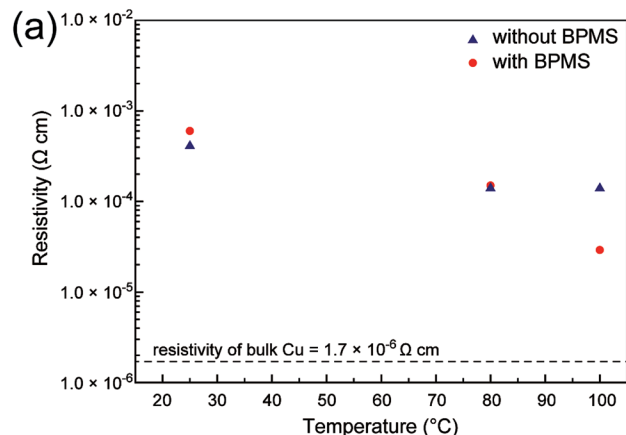


Fig. 4 (a) Resistivities of hot-pressed Cu pellets with (circles: ●) and without (triangles: ▲) BPMS as the thermal acid generator. The resistivity of bulk copper is  $1.7 \times 10^{-6} \text{ } \Omega \text{ cm}$  and is displayed as the dashed line. (b) XRD patterns of hot-pressed Cu pellets with BPMS. The (111) plane of  $\text{Cu}_2\text{O}$  is marked as closed circle (●).

Hot pressing was also carried out in the presence of BPMS. In the presence of BPMS as the proton generator, the pellets pressed at  $25$  and  $80 \text{ }^\circ\text{C}$  showed similar resistivities as the pellets obtained without BPMS ( $6.0 \times 10^{-4}$  and  $1.5 \times 10^{-4} \text{ } \Omega \text{ cm}$ , respectively). However, the resistivity was dramatically decreased to  $2.9 \times 10^{-5} \text{ } \Omega \text{ cm}$  in the case of the pressing temperature of  $100 \text{ }^\circ\text{C}$ . This result indicates that the BDVE surrounding Cu particles was decomposed at  $100 \text{ }^\circ\text{C}$  by the acid derived from BPMS, as shown in Fig. 3, resulting in the densely packed Cu particles in the pellet with metal–metal direct contacts (see the SEM image in Fig. S3†).

Fig. 4b shows the XRD patterns of the pellets pressed with BPMS. It is shown that the surface of the Cu particles was partially oxidized to  $\text{Cu}_2\text{O}$ , after being heated and pressed in air at  $80 \text{ }^\circ\text{C}$  and  $100 \text{ }^\circ\text{C}$  for 30 min. The Cu pellet prepared at  $100 \text{ }^\circ\text{C}$  contained 4 wt% of  $\text{Cu}_2\text{O}$ , as per calculation using the reference intensity ratio (RIR) method.<sup>47</sup> This partial oxidation can be explained by the two reasons. TGA-DTA measurement of BDVE-stabilized Cu fine particles (dashed line of Fig. 2 and S2†) indicates that they began to be oxidized at *ca.*  $87 \text{ }^\circ\text{C}$ . The other is decomposition of BDVE by BPMS at high temperatures. Despite the oxidation, Cu pellets showed a low resistivity of  $2.9 \times 10^{-5} \text{ } \Omega \text{ cm}$ .



cm at pressing temperature of 100 °C in the presence of BPMS, which is in accordance with the low-temperature decomposition of BDVE. This resistivity value is extremely low even though the most particles shall be remained covered by BDVE that is not degraded, only 17 times higher than bulk copper.

After pressing at 100 °C, the pellet was pulverized into powder and its TGA-DTA measurement was performed (solid lines of Fig. 2 and S2†). Comparing with the curves of the as-prepared BDVE-stabilized Cu fine particles, the pellet shows better anti-oxidation ability. The Cu particles in the pellet began to be oxidized at 120 °C, that is, 33 °C higher than the as-prepared Cu fine particles BDVE can be decomposed at *ca.* 100 °C in the presence of BPMS. However, all decomposed components were not evaporated during pressing. As indicated in Fig. 5, Cu fine particles in the pellet prepared at 100 °C were covered by BDVE polymer residues. This image indicates that the polymer residues after pressing densely covered the surface of particles and necking parts. This phenomenon strongly prevents oxidation of copper in the pellet as observed in the TGA-DTA curves in Fig. 2 and S2.†

Corrosion tests of these hot-pressed conductive Cu pellets revealed that the resistivities of pellets could last for 8 days in the oppressive condition of 85 °C and 85% relative humidity as shown in Fig. 6. This good anti-corrosion stability can be attributed to the polymer layer on Cu particles and neckings as shown in Fig. 5. This low-temperature proton-aided hot pressing is a quite useful process to obtain highly conductive copper pellets.

### Preparation of the Cu fine-particle ink and conductive films via acid-assisted sintering

Printing electronics using metal-particle inks or pastes has been attracted much attention so far as an ecological method to realize highly conductive electronic circuits. Therefore, we tried to prepare an ink containing above the obtained BDVE-stabilized Cu fine particles.

BDVE-stabilized Cu fine particles were re-dispersed into 50 wt% of  $\alpha$ -terpineol to form an electro-conductive ink. 10 wt% of

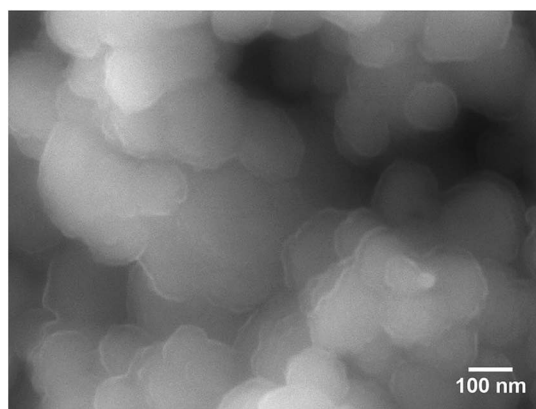


Fig. 5 SEM image of the fracture surface of a Cu fine particle pellet pressed at 100 °C. Cu fine particles are covered by BDVE polymer residues.

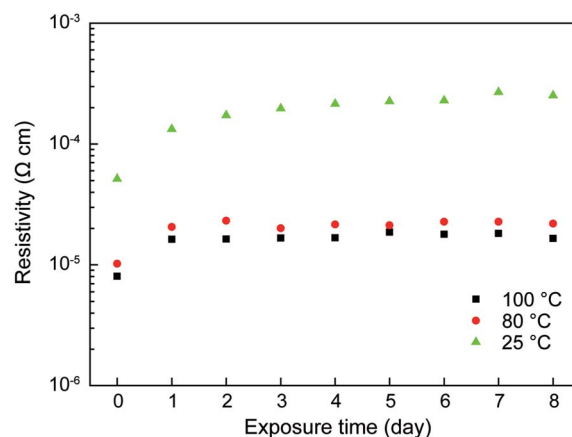


Fig. 6 Corrosion tests of the hot-pressed conductive Cu pellets with BPMS. The condition of the test was 85 °C and 85% relative humidity. The resistivities were increased after 1 day in the condition. However, the resistivities lasted for other 7 days without any obvious increase.

formic acid as the proton generator was introduced into the ink just before application on substrates. Then, the ink was printed onto a glass and an Al<sub>2</sub>O<sub>3</sub> substrates by using the doctor blade method. After printing, the Cu film was dried at 40 °C under N<sub>2</sub> flow. The obtained Cu film was annealed at 150 °C in 3% H<sub>2</sub> in N<sub>2</sub> gas for 2 h. Fig. 7a shows the XRD patterns of Cu film on the glass before and after annealing. The Cu film was not oxidized during annealing. The surface of the Cu film was observed by SEM (Fig. 7b). In this image, both the necking structures

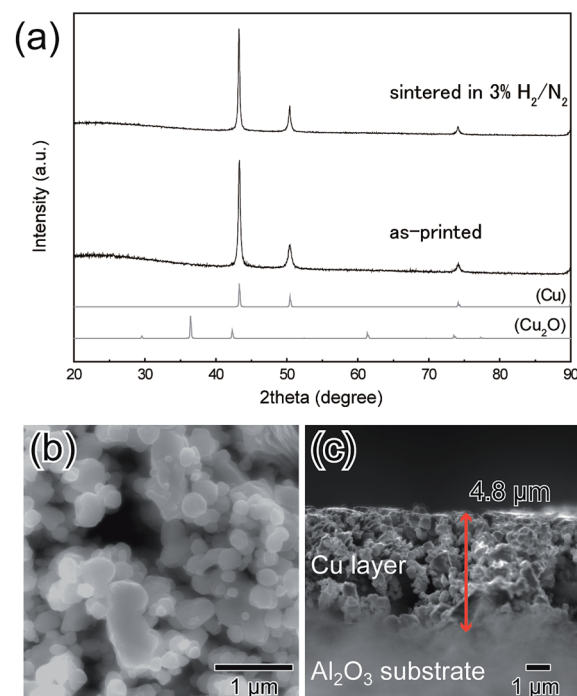


Fig. 7 (a) XRD patterns of Cu films on a glass before and after sintering. (b) SEM image of the Cu film sintered at 150 °C in 3% H<sub>2</sub> in N<sub>2</sub> gas. (c) Cross-sectional SEM image of (b). The thickness of film was 4.8 μm marked as red arrowed line.



between copper particles and the inter-particle connections could be observed. The thickness of annealed Cu film was 4.8  $\mu\text{m}$ , as observed in Fig. 7c. After annealing in 3%  $\text{H}_2$  in  $\text{N}_2$  gas, the sheet resistance and resistivity for the resulting film were  $0.18 \Omega \text{sq}^{-1}$  and  $8.5 \times 10^{-5} \Omega \text{cm}$ , respectively. As the decomposed BDVE fragments formed by the addition of formic acid were evaporated at 150  $^\circ\text{C}$ , the copper–copper direct contact area between particles increased. The Cu film was also annealed at 100  $^\circ\text{C}$  in 3%  $\text{H}_2$  in  $\text{N}_2$  gas for 2 h, but the obtained copper layer was unfortunately an insulator. This is because that decomposed fragments of BDVE were not evaporated at 100  $^\circ\text{C}$  as shown in Fig. 3.

As indicated in Fig. 3, BPMS works as a good thermal proton generator. As indicated above, hot-pressed Cu pellets (at 100  $^\circ\text{C}$ ) assisted by BPMS showed low resistivity of  $2.9 \times 10^{-5} \Omega \text{cm}$ . We have also prepared a Cu ink with 1 wt% of BPMS, and copper particle layers were prepared by the doctor blade method. Surprisingly, the layers showed non-conductive property after sintering even at 150  $^\circ\text{C}$  in 3%  $\text{H}_2$  in  $\text{N}_2$  gas for 2 h.

At this moment, we have not obtained clear evidences to explain the difference between the favourable proton generators in the two cases. BPMS decomposes BDVE at a much lower temperature than formic acid does. The decomposition of BDVE to easily evaporated fragments as a result of hot pressing is very important because the contacts between copper fine particles can be easily generated by the external pressure when no organic molecules are found on the surface. In contrast, without an external pressure, copper fine particles cannot move easily when the particles lose the outer layer. However, when they are covered by polymers, at temperatures above the glass transition temperature of the polymer, copper particles can move slightly and connect the particle surfaces. Therefore, interparticle connections could be formed in the case of addition of formic acid due to a relatively high pyrolysis temperature as shown in Fig. 3.

In this sintering process, the evaporation of polymer fragments and the formation of interparticle contacts are the most important factors to achieve electro-conductivity. Thus, sintering with formic acid makes the Cu film electro-conductive.

## Conclusions

In summary, we have used a polymer, which undergoes proton-assisted degradation, to stabilize copper fine particles for the first time. Proton-assisted single-step sintering of polymer-stabilized Cu fine particles was successfully performed at a low temperature to obtain highly conductive Cu pellets and films. In fact, only 0.7 wt% of polymer layer on the surface of particles could provide Cu fine particles with the anti-oxidation ability. In our system, acids promote the hydrolysis of polymer and the fragments of decomposed polymer can be evaporated at a low temperature. In the presence of a thermal acid generator, the Cu conductive pellet was obtained by hot pressing at 100  $^\circ\text{C}$ . In spite of oxidation of the surface layer, Cu particles were densely packed and the resultant pellets showed the low resistivity of  $2.9 \times 10^{-5} \Omega \text{cm}$ . The hot pressed pellets showed better anti-oxidative property than the as-prepared Cu fine particles.

Also, the hot pressed pellets showed good anti-corrosion stability at 85  $^\circ\text{C}$  and 85% of relative humidity. Furthermore, formic acid can decompose the polymer. After sintering in the presence of reductive gas and formic acid, a conductive Cu film with the low resistivity of  $8.5 \times 10^{-5} \Omega \text{cm}$  was successfully prepared. In this sintering process, the evaporation of polymer fragments and the formation of dense inter-particle contacts are the key factors to realize high electro-conductivity. The decomposable-polymer-protected Cu particles are therefore promising candidates for obtaining the electro-conductive films and pellets *via* low-temperature sintering. This novel strategy could enable the application of low-temperature sintering of relatively large fine particles for use in printed electronics.

## Acknowledgements

This work is partially supported by Hokkaido University (to TY). MTN acknowledges the financial support from F3 program of Hokkaido University. TY also thanks a partial support from Shinsei Foundation, Murata Foundation and Network Joint Research Center for Materials and Devices, Japan.

## Notes and references

- 1 M.-C. Daniel and D. Astruc, *Chem. Rev.*, 2004, **104**, 293–346.
- 2 N. Toshima and T. Yonezawa, *New J. Chem.*, 1998, **22**, 1179–1201.
- 3 K. E. Sapsford, W. R. Algar, L. Berti, K. B. Gemmill, B. J. Casey, E. Oh, M. H. Stewart and I. L. Medintz, *Chem. Rev.*, 2013, **113**, 1904–2074.
- 4 Y. Ishida, T. Sumi and T. Yonezawa, *New J. Chem.*, 2015, **39**, 5895–5897.
- 5 Y.-H. Yang, C.-H. Liu, Y.-H. Liang, F.-H. Lin and K. C.-W. Wu, *J. Mater. Chem. B*, 2013, **1**, 2447–2450.
- 6 S. Karmakar, K. Kumar, R. Rinaldi and G. Maruccio, *J. Phys.: Conf. Ser.*, 2011, **292**, 012002.
- 7 A. N. Shipway, E. Katz and I. Willner, *ChemPhysChem*, 2000, **1**, 18–52.
- 8 T. Yonezawa, S. Takeoka, H. Kishi, K. Ida and M. Tomonari, *Nanotechnology*, 2008, **19**, 147506.
- 9 K. Nomura, H. Ohta, A. Takagi, T. Kamiya, M. Hirano and H. Hosono, *Nature*, 2004, **432**, 488–492.
- 10 S. H. Ko, H. Pan, C. P. Grigoropoulos, C. K. Luscombe, J. M. J. Fréchet and D. Poulidakos, *Nanotechnology*, 2007, **18**, 345202.
- 11 M. Berggren, D. Nilsson and N. D. Robinson, *Nat. Mater.*, 2007, **6**, 3–5.
- 12 F. N. Ishikawa, H.-K. Chang, K. Ryu, P.-C. Chen, A. Badmaev, L. G. De Arco, G. Shen and C. Zhou, *ACS Nano*, 2009, **3**, 73–79.
- 13 W. Cui, W. Lu, Y. Zhang, G. Lin, T. Wei and L. Jiang, *Colloids Surf., A*, 2010, **358**, 35–41.
- 14 M. J. Cotts, M. B. Cortie, M. J. Ford and A. M. McDonagh, *J. Phys. Chem. C*, 2009, **113**, 1325–1328.
- 15 T. Bakhishev and V. Subramanian, *J. Electron. Mater.*, 2009, **38**, 2720–2725.
- 16 J. R. Greer and R. A. Street, *Acta Mater.*, 2007, **55**, 6345–6349.



- 17 B. Y. Ahn, E. B. Duoss, M. J. Motala, X. Y. Guo, S. I. Park, Y. J. Xiong, J. Yoon, R. G. Nuzzo, J. A. Rogers and J. A. Lewis, *Science*, 2009, **323**, 1590–1593.
- 18 B. Y. Ahn, D. J. Lorang and J. A. Lewis, *Nanoscale*, 2011, **3**, 2700–2702.
- 19 H.-H. Lee, K.-S. Chou and K.-C. Huang, *Nanotechnology*, 2005, **16**, 2436–2441.
- 20 T. Yonezawa, *Kobunshi Ronbunshu*, 2013, **70**, 684–692.
- 21 Y. Jianfeng, Z. Guisheng, H. Anming and Y. N. Zhou, *J. Mater. Chem.*, 2011, **21**, 15981–15986.
- 22 Y. Zhang, P. Zhu, G. Li, T. Zhao, X. Fu, R. Sun, F. Zhou and C.-P. Wong, *ACS Appl. Mater. Interfaces*, 2014, **6**, 560–567.
- 23 R. Sierra-Ávila, M. Pérez-Alvarez, G. Cadenas-Pliego, C. A. Ávila-Orta, R. Betancourt-Galindo, E. Jiménez-Regalado, R. M. Jiménez-Barrera and J. G. Martínez-Colunga, *J. Nanomater.*, 2014, **2014**, 361791.
- 24 M. Tomonari, K. Ida, H. Yamashita and T. Yonezawa, *J. Nanosci. Nanotechnol.*, 2008, **8**, 2468–2471.
- 25 T. Narushima, H. Tsukamoto and T. Yonezawa, *AIP Adv.*, 2012, **2**, 042113.
- 26 T. Yonezawa, H. Tsukamoto and M. Matsubara, *RSC Adv.*, 2015, **5**, 61290–61297.
- 27 M. Matsubara, T. Yonezawa and H. Tsukamoto, *Bull. Chem. Soc. Jpn.*, DOI: 10.1246/bcsj.20150305, in press.
- 28 D. Deng, Y. Cheng, Y. Jin, T. Qi and F. Xiao, *J. Mater. Chem.*, 2012, **22**, 23989–23995.
- 29 W. Chen, D. Deng, Y. Cheng and F. Xiao, *J. Electron. Mater.*, 2015, **44**, 2479–2487.
- 30 C.-Y. Tsai, W.-C. Chang, G.-L. Chen, C.-H. Chung, J.-X. Liang, W.-Y. Ma and T.-N. Yang, *Nanoscale Res. Lett.*, 2015, **10**, 357.
- 31 Y. Yong, T. Yonezawa, M. Matsubara and H. Tsukamoto, *J. Mater. Chem. C*, 2015, **3**, 5890–5895.
- 32 H. Nishikawa, S. Mikami, K. Miyake, A. Aoki and T. Takemoto, *Mater. Trans.*, 2010, **51**, 1785–1789.
- 33 Y. Kobayashi and T. Sakuraba, *Colloids Surf., A*, 2008, **317**, 756–759.
- 34 A. Kamyshny, J. Steinke and S. Magdassi, *Open Appl. Phys. J.*, 2011, **4**, 19–36.
- 35 A. Yabuki, N. Arriffin and M. Yanase, *Thin Solid Films*, 2011, **519**, 6530–6533.
- 36 A. Yabuki and S. Tanaka, *Mater. Res. Bull.*, 2012, **47**, 4107–4111.
- 37 A. Yabuki, Y. Tachibana and I. W. Fathona, *Mater. Chem. Phys.*, 2014, **148**, 299–304.
- 38 D.-H. Shin, S. Woo, H. Yem, M. Cha, S. Cho, M. Kang, S. Jeong, Y. Kim, K. Kang and Y. Piao, *ACS Appl. Mater. Interfaces*, 2014, **6**, 3312–3319.
- 39 Y. Farraj, M. Grouchko and S. Magdassi, *Chem. Commun.*, 2015, **51**, 1587–1590.
- 40 Y. Hu, B. An, C. Niu, W. Lv and Y. Wu, *Int. Conf. Electron. Packag. Technol. High Density Packag., 15th*, 2014, 1565–1567, DOI: 10.1109/ICEPT.2014.6922953.
- 41 C. Paquet, R. James, A. J. Kell, O. Mozenon, J. Ferrigno, S. Lafreniere and P. R. L. Malenfant, *Org. Electron.*, 2014, **15**, 1836–1842.
- 42 G. Qin, A. Watanabe, H. Tsukamoto and T. Yonezawa, *Jpn. J. Appl. Phys.*, 2014, **53**, 096501.
- 43 C. Engineer, J. Parikh and A. Raval, *Trends Biomater. Artif. Organs.*, 2011, **25**, 79–85.
- 44 S. P. Lyu and D. Untereker, *Int. J. Mol. Sci.*, 2009, **10**, 4033–4065.
- 45 Y. Ikeda and H. Tsuji, *Macromol. Rapid Commun.*, 2000, **21**, 117–132.
- 46 M. Abtewa and G. Selvaduray, *Mater. Sci. Eng.*, 2000, **27**, 95–141.
- 47 R. L. Snyder, *Powder Diffr.*, 1992, **7**, 186–193.

